Supplement of

Were early Archean carbonate factories major carbon sinks on the juvenile Earth?

Xiang, Wanli[1, 2], Duda, Jan-Peter[2], Pack, Andreas[3], van Zuilen, Mark[4], Reitner, Joachim[2, 5]

[1] College of Tourism and Geographical Science, Leshan Normal University, Leshan, 614000, China.
[2] Department of Geobiology, University of Göttingen, Göttingen, 37077, Germany.
[3] Department of Geochemistry and Isotope Geology, University of Göttingen, Göttingen, 37077, Germany.
[4] CNRS-UMR6538 Laboratoire Geo-Ocean, Institut Universitaire Européen de la Mer (IUEM), Université de Bretagne Occidentale, Plouzané, 29280, France.
[5] Göttingen Academy of Science and Humanities in Lower Saxony, Göttingen, 37073, Germany.

Correspondence to Reitner Joachim (jreitne@gwdg.de)

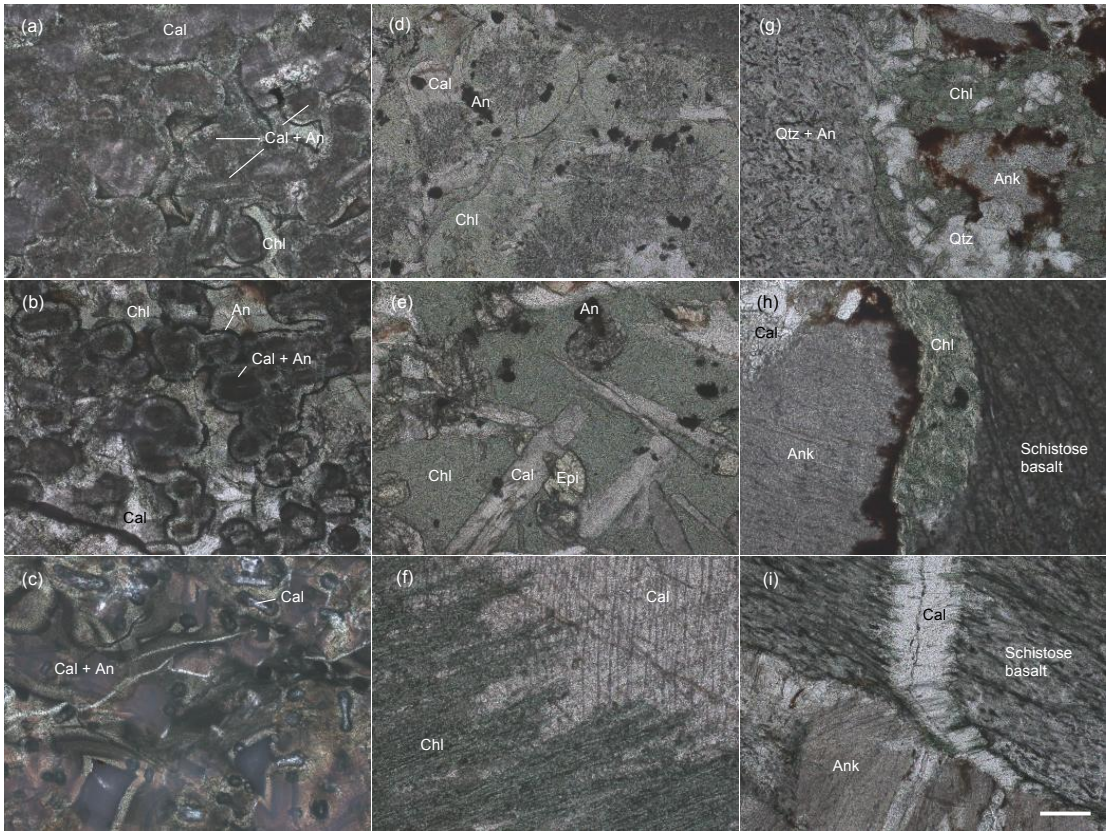

Figure S1: Thin section photographs of interstitial carbonates and host basalts. (a–c) Decreasing sizes and density of carbonatized variolites in basaltic margin. (d) Breakup of the variolites resulting in anatase particles and calcite laths. (e) Secondary minerals include calcite, chlorite, anatase and epidote. (f–h) Migration of chlorite into interstitial space of basalt. (i) Schistose basalt cut by a calcite vein formed through brittle deformation. (a–f) are from the Apex Basalt, (g–i) from the Mount Ada Basalt. All photos were taken under plane-polarized light. Scale bar in (i) equals to 200 µm and applies to all photos. Abbreviations: Cal- calcite, An- anatase, Chl- chlorite, Qtz- quartz, Epi- epidote, Ank-ankerite.

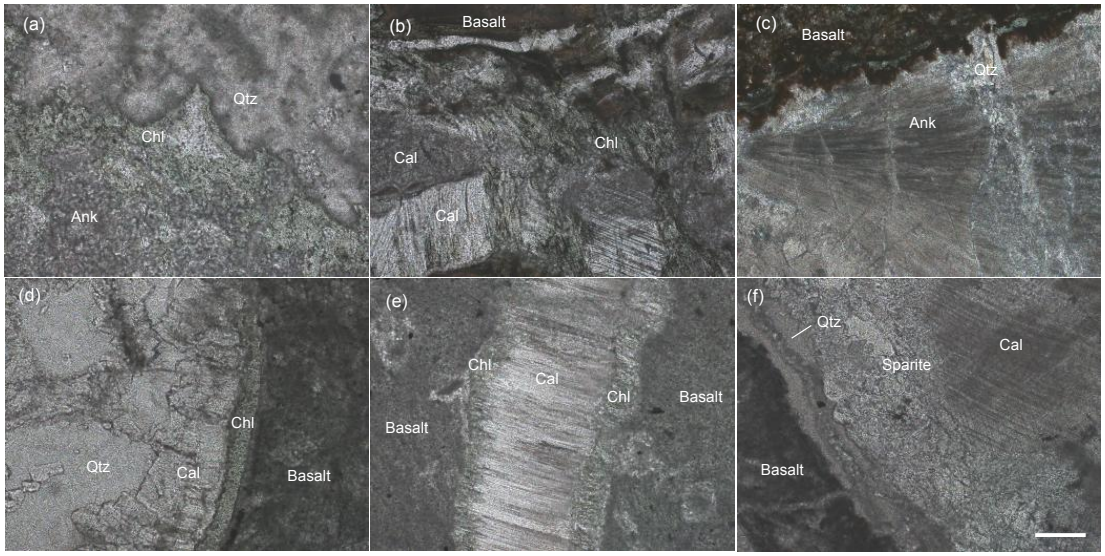

Figure S2: Thin section photographs showing the secondary carbonate facies of interstitial carbonates. (a) Microcrystalline ankerite (Ank) and quartz (Qtz) are rare and observed at the basalt margin, mixing with chlorite (Chl) and anatase particles (~nm). (b) Blocky calcite is the primary carbonate generation within concentric syngenetic veins in pillow basalt (near the cross A22-vein-2 in Fig. 3a). It was cemented by fibrous isopachous calcite during tectonic events. (c) A relict structure of acicular crystal-fan in ankerite. (d) Sharp contacts between edge of basalt, chlorite and isopachous calcite. (e) Contact in parallel veins within basalt, similar to those shown in (d). (f) Contacts of calcite in interspaces are distinct to those shown in (d), indicating that the studied calcite (D-2) formed within a wide fracture (therefore addressed as "fracture-filling calcite"). (a, b) are from Apex Basalt, (c) from Mount Ada Basalt, and (d–f) from the Dresser Formation. Photos were taken under plane-polarized light. The scale bar in (f) corresponds to 200 µm and applies to all photos.

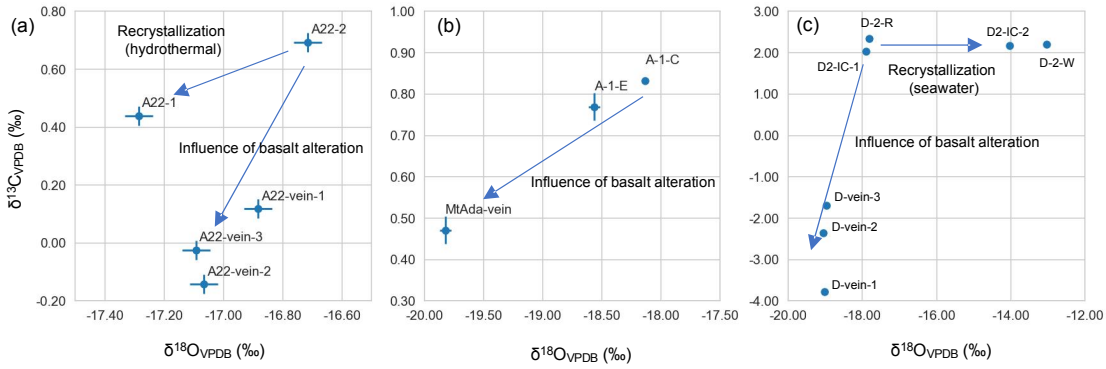

Figure S3: Cross-plots of $\delta^{13}C$ and $\delta^{18}O$ date for the interstitial carbonates and veinlet carbonates in samples (a) A22, (b) MtAda-1 and (c) D-2. The relative positions are marked in Figs. 3 and 5, respectively.

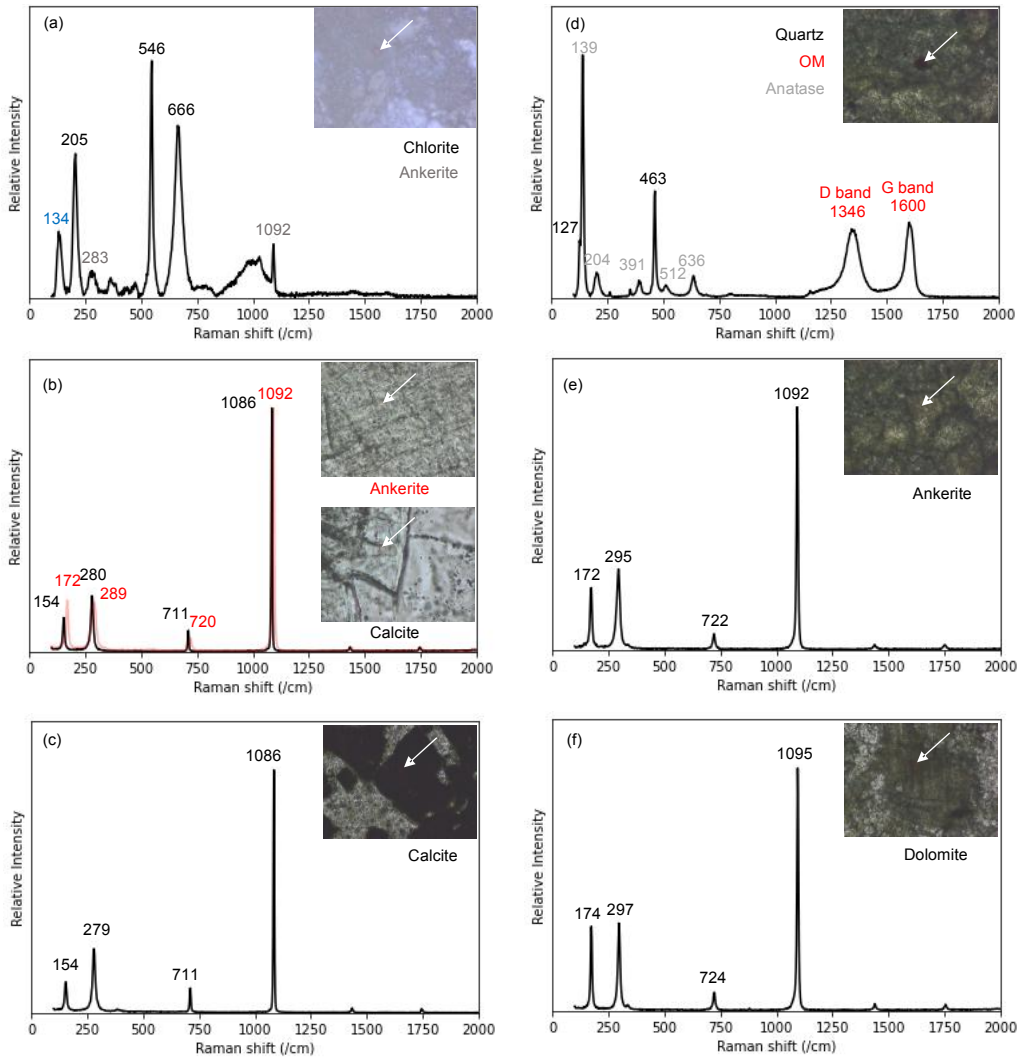

Figure S4: Raman spectra for mineral assemblages in the studied early Archean carbonates. (a) Minor ankerite mixing with chlorite at the margin of pillow basalt from the Apex Basalt. (b) Interstitial carbonates from the Mount Ada Basalt consist of ankerite overgrown by calcite. (c) Carbonate rhombs of the bedded carbonate from the Dresser Formation consist of calcite. (d) Anatase and quartz with encapsulated organic matter are interbedded with (e) ankerite of the bedded carbonate from the Euro Basalt. (f) Stromatolite of the Strelley Pool Formation mainly consist of dolomite.

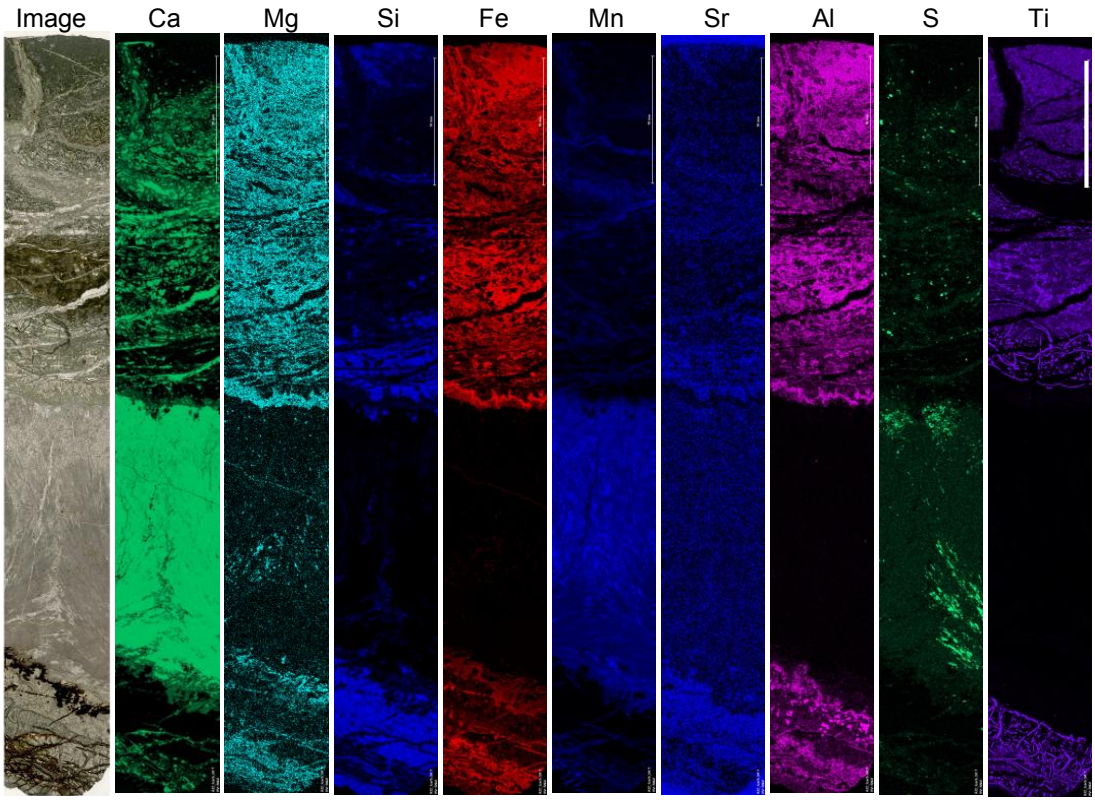

Figure S5: False-color element images of µXRF mappings, showing element distributions in interstitial carbonates from the Apex Basalt. The scale bar is 10 mm.

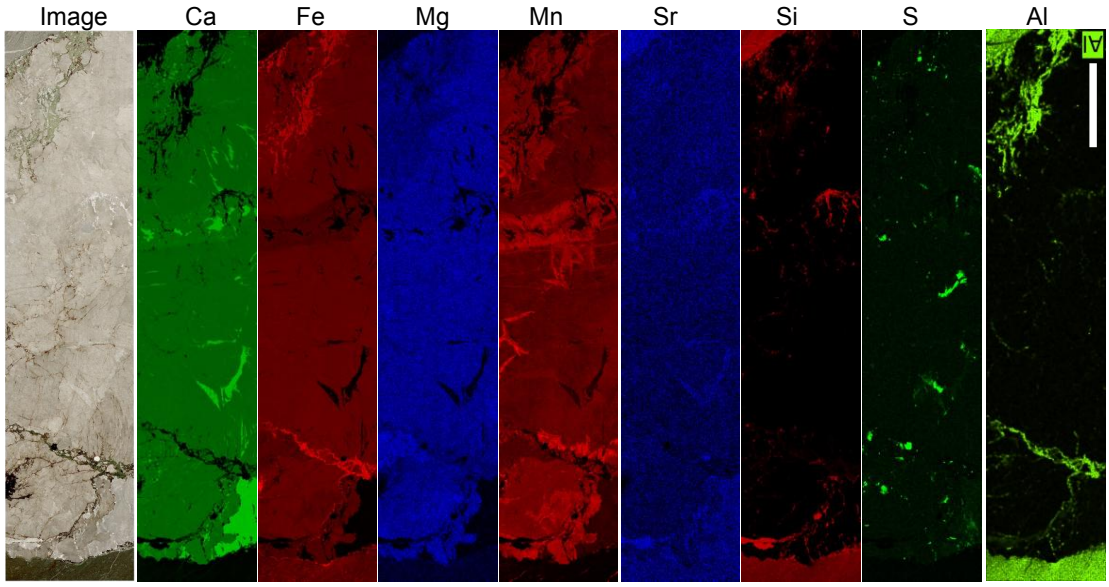

Figure S6: False-color element images of µXRF mappings, showing element distributions in interstitial carbonates from the Mount Ada Basalt. The scale bar is 10 mm.

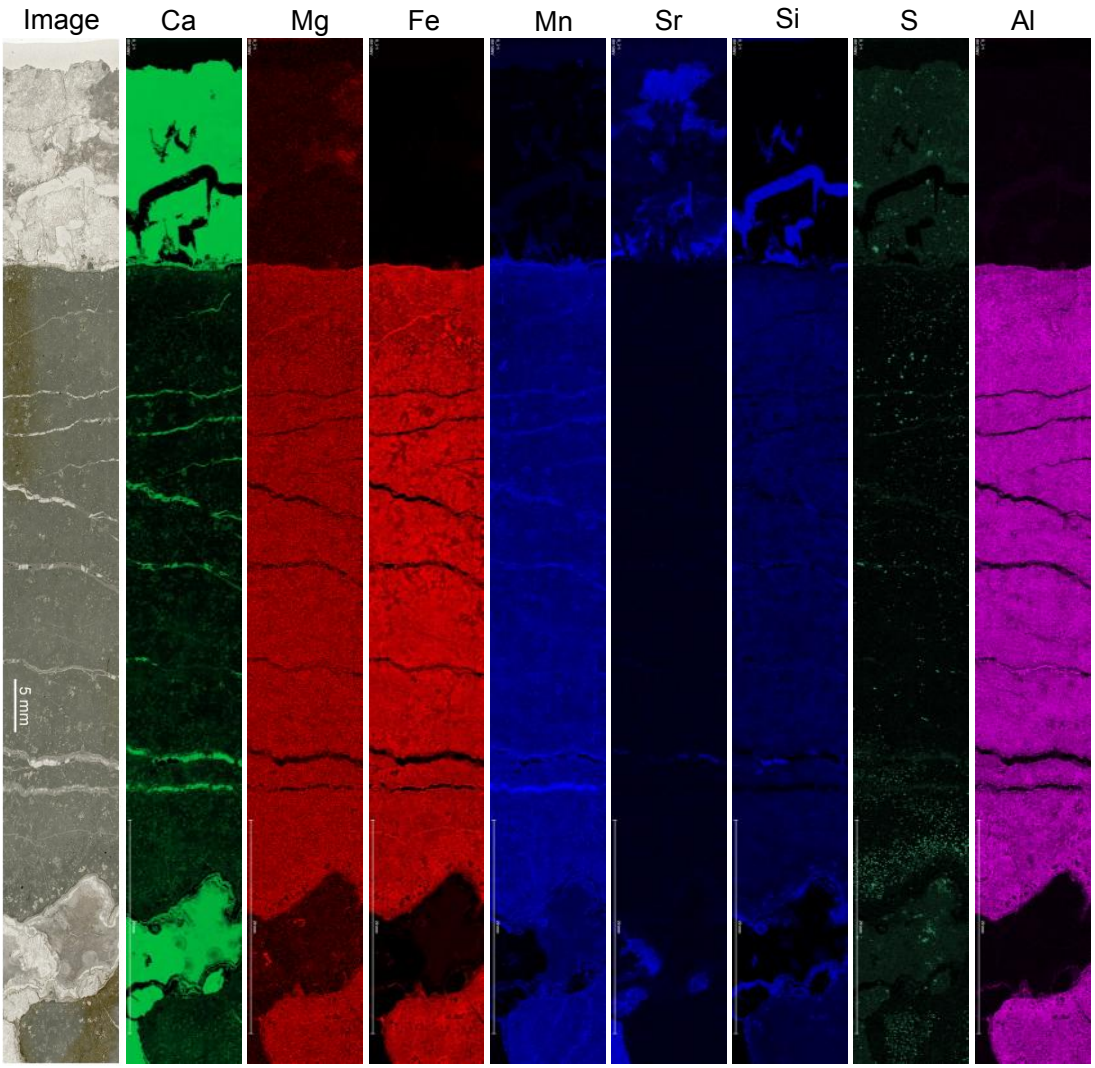

Figure S7: False-color element images of µXRF mappings, showing element distributions in interstitial carbonates from the Middle Basalt Member of Dresser Formation.

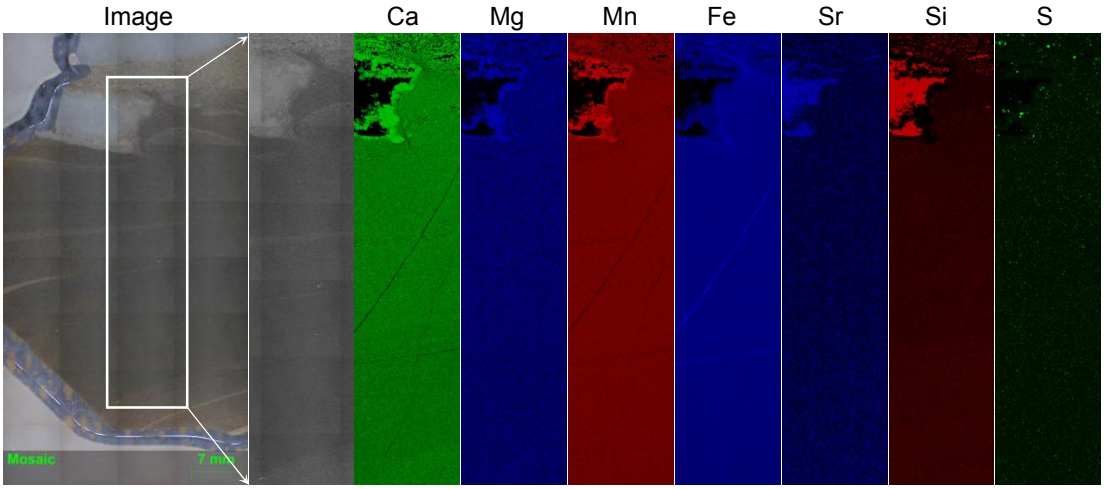

Figure S8: False-color element images of µXRF mappings, showing element distributions in the laminated micritic sedimentary carbonate of the Dresser Formation.

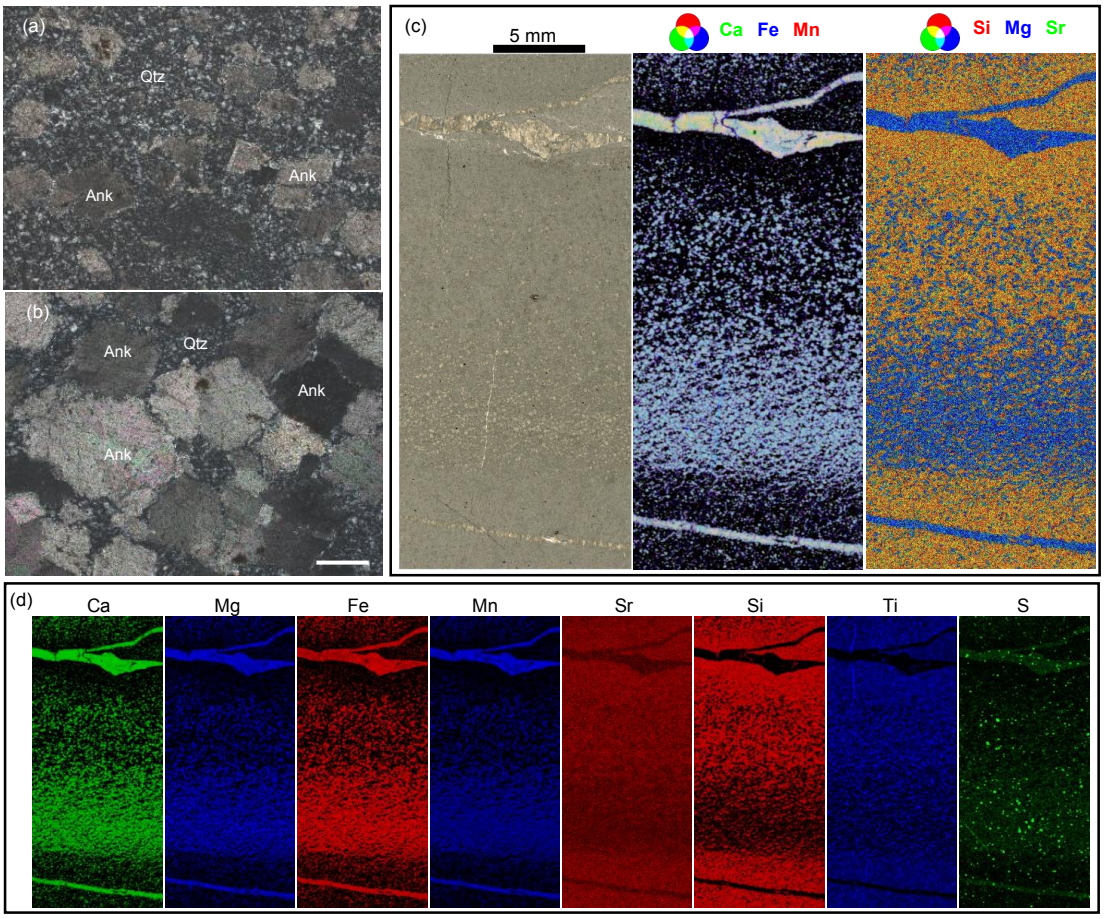

Figure S9: Images of the bedded sedimentary chert-carbonate from the Euro Basalt. (a) Subhedral to anhedral ankerite (Ank) rhombs in the microcrystalline quartz (Qtz) matrix in the upper part of a layer. (b) Ankerite rhombs are larger in the lower part of a layer, and experienced pressure dissolution. (c) False-color overlapping images show the size-grading of Fe- and Mn-enriched dolomite crystals and veins in a chert matrix. (d) False-color element images of µXRF mappings. (a) and (b) were taken under cross-polarized light; the scale bar corresponds to 200 µm.

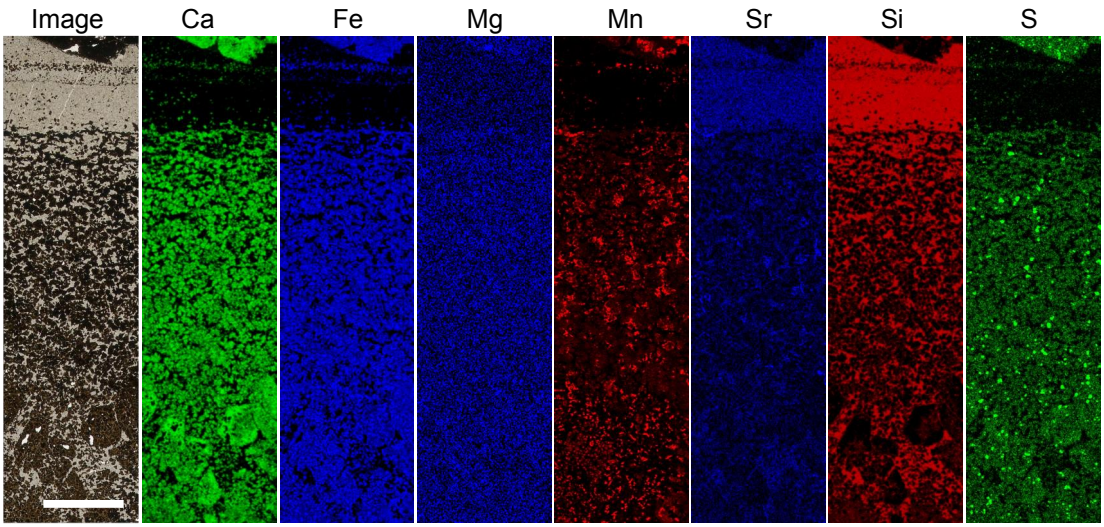

Figure S10: False-color element images of µXRF mappings, showing element distribution in the Dresser bedded carbonate. The scale bar is 5 mm.

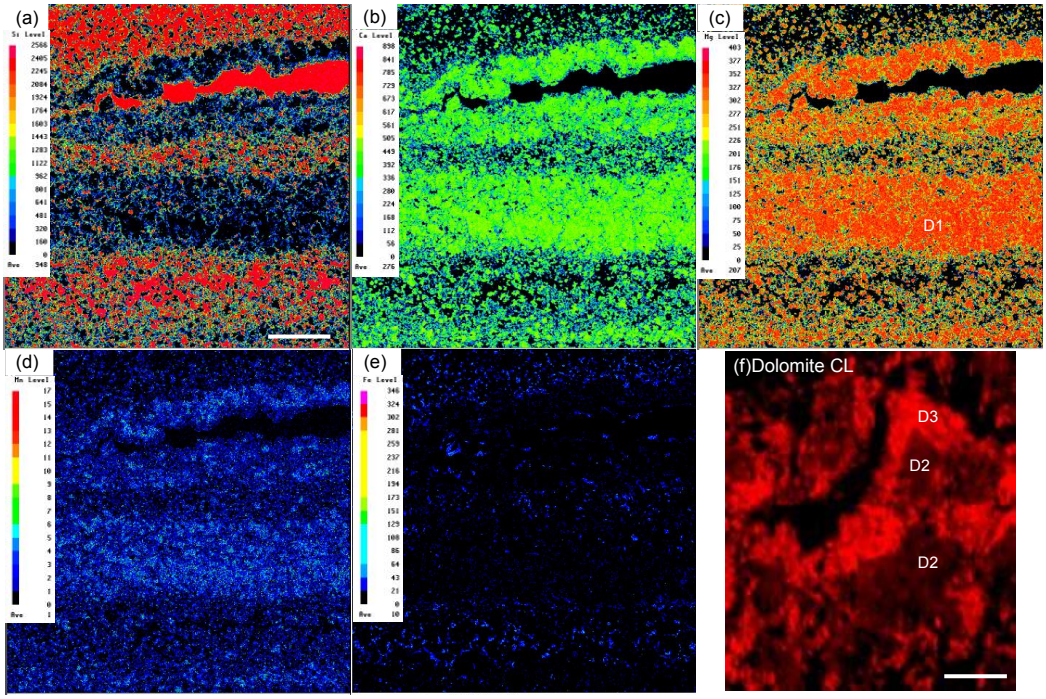

Figure S11: Images of the stromatolitic carbonates from the Strelley Pool Formation. EPMA mappings of (a) Si, (b) Ca, (c) Mg, (d) Mn, and (e) Fe, highlighting silicified laminae of Mn-enriched dolomites. (f) CL image of dolomite, illustrating the presence of a first generation (D1) followed by two recrystallized generations (D2 and D3). (a–e) EPMA analyses were conducted at 15 kV with a probe diameter of 10 µm using a JEOL 8900 RL electron microprobe instrument by Dr. Andreas Kronz (Department of Mineralogy, University of Göttingen). The scale bar in (a) corresponds to 2 mm and also applies to (b–e); the scale bar in (f) is 25 µm.